Journal of Population Therapeutics
& Clinical Pharmacology

RESEARCH ARTICLE
DOI: 10.53555/jptcp.v31i7.7320

INCORPORATION OF CDS NANOPARTICLES INTO PMMA MATRIX AND THEIR PHOTOCATALYTIC RESPONSE AGAINST METHYLENE BLUE

Huma Tareen[1], Farrukh Bashir[1*], Irum Javid[2], Naheed Sajjad[3], Zile Huma[4], Muhammad Riaz[5], Khurrum Shazad Buzdar[6], Muhammad Aamir Raza[6], Uzma Jabeen[1]

[1]Department of Chemistry, Sardar Bahadur Khan Women, University, Quetta-87300, Pakistan
[2]Department of Biochemistry, Sardar Bahadur Khan Women, University, Quetta-87300, Pakistan
[3]Department of Biotechnology, Sardar Bahadur Khan Women, University, Quetta-87300, Pakistan
[4]Department of Zoology, Sardar Bahadur Khan Women, University, Quetta-87300, Pakistan
[5]Department of Allied Health Sciences, University of Sargodha, Sargodha-40100, Pakistan
[6]Pakistan Council of Science and Industrial Research Laboratories Complex, Quetta-87300, Pakistan

***Corresponding Author:** Dr. Farrukh Bashir:
*Email Address: farrukh_chem@yahoo.com

Abstract

Thin films of cadmium sulphide/poly methyl methacrylate (CdS/PMMA) were synthesized by the using solution casting method. This method was used due to the hydrophilic and hydrophobic compatibility of metal sulphide with PMMA matrix. The fabricated films were characterized by using X-ray diffraction (XRD), Fourier-transform infrared (FTIR) and Ultraviolet-visible (UV-Vis) spectroscopy. The photocatalytic activity of these films was carried out by using methylene blue solution as a water pollutant. Results revealed that as the content of CdS was increased in the polymer matrix, the band gap values became narrower (2.3 eV for sample F). Furthermore, the thin film of 0.8g CdS/PMMA exhibited the highest and fastest rate of photocatalytic degradation (99 % in 240 minutes) among all the composites. These results are attributed to the narrow band gap, higher adsorption capacity and good electron acceptability of CdS. Hence, toxic waste products produced by different industries could be removed by using CdS/PMMA photocatalysts.

Keywords: Poly methyl methacrylate, Photocatalysis, Methylene blue, Band gap energy.

Introduction

Methylthioninium Chloride, formally known as methylene blue (MB) is a lipophilic azo compound with a dark bluish-green color and crystalline structure. In 1876, this compound was synthetically synthesized for the textile industry (textile manufacturer Heinrich Caro), however, its use in laboratory and medication began only 14 years later. MB as a diagnostic substance has several applications in medication like staining cell cultures, DNA detection, visualizing microbiological structures, photodynamic therapy, fungal and parasitic infections, antimalarial agent, treatment of methemoglobinemia, an antidote for cyanide poisoning. As its mechanism of action in human medicinal practice is not precisely known therefore US FDA has issued a safety warning and its higher dose may cause diseases like abdominal pain, dyspnea, precordial pain and reversible staining of skin [1,2]. MB is commonly used in the dye industry for coloring silk, cotton, wool, silk and paper and causing water contamination (due to its stable water solubility) which is ultimately hazardous for life [3-5]. The number of articles published on the removal of MB has been increasing continuously via adsorption and bioremediation [6-8], however, articles on photodegradation of MB via polymer composites are very few.

Transition metals that belong to II-VI semiconductor group, have fascinated the interest of researchers due to their excellent luminescent and optical properties. Cadmium sulphide (CdS) nanoparticles are one of them, that are being studied due to their n-type photo sensible semiconduction and prompt response towards the light with 2.42 eV direct band gap [9,10]. These nanoparticles are also known as fluorescent nanoparticles [11] and they have been synthesized by different methods like, hydrothermal, sol-gel, chemical co-precipitation, sonochemical, and so on [10,12]. They have several applications like in photodetectors, light emitting diodes, photocatalyts, biological indicators, sensors, transistors, solar cells, etc. [11,13,14]. In the last few years, CdS nanoparticles have been used as a promising candidate in photochemical reactions, as they can illuminate visible light and enable the excitation of the electrons from the valence to the conduction band. However, their applications in photochemical reactions are limited because of their degradation when exposed to the atmosphere, low surface area, lack of active sites and low efficiency in utilizing UV light. These limitations result in the fast recombination of the excited electrons and thus decrease the quantum efficiency. To overcome these limitations two methods have been reported; coupling of these nanoparticles with nonmetals or polymers and hybrid formation with different semiconducting materials [15,16].

Doping of CdS with polymer matrix has appealed to the attention of researchers, as their combination results in several new photocatalytic and photoelectric applications by increasing the rate of photogenerated excited electron/hole pairs separations [17]. Poly methyl methacrylate (PMMA) has been used in many technological and productive areas because of its eco-friendly, low-cost effective, optical transparency, and unique mechanical and physio-chemical characteristics. It can reduce the recombination rate of photogenerated electron-hole pairs by prolonging their center life However, its thermal instability and lack of UV light filtration have reduced its utilization globally but these drawbacks can be reduced by its combination with semiconductors [18]. Literature is reported where incorporation of CdS and PMMA had not only improved the properties of CdS nanoparticles but also enhanced the mechanical, electrical and optical properties of PMMA dramatically and made them useful in photocatalytic and photoconductivity applications. Effective dispersion of CdS nanoparticles in the PMMA matrix enhances the transition temperature of the matrix. Similarly, PMMA serves as a protective shield for these nanoparticles by encapsulating them and protecting them from their direct exposure to any external environment. It is also observed that being transparent, PMMA allows the photons to interact with these nanoparticles through penetration [9]. Methods like solution casting [18,19], and embedding by using a photocuring process [20] have been employed for the synthesis of CdS/PMMA composites.

The present research is focused on the investigation of photocatalytic properties of CdS/PMMA composites by using different concentrations of CdS nanoparticles. The novelty of this work lies in the photodegradation of methylene blue by using CdS/PMMA composite in an alkaline medium by using a few drops of barium hydroxide solution to keep the observed system at pH equal to 10. Characterization of these composites was done by using X-ray diffraction (XRD) for crystalline properties, FTIR for molecular interactions and ultraviolet-visible (UV-Vis) spectrophotometer for adsorption and optical band gap studies.

Methodology

Three steps were followed for the present study.

Synthesis of CdS nanoparticles

CdS nanoparticles were prepared at room temperature by using cadmium sulphate ($CdSO_4$) and sodium sulphide (Na_2S) chemicals as main precursors. Equimolar (0.1M) aqueous solutions of $CdSO_4$ and Na_2S were prepared separately in 25 mL of deionized water at constant stirring for 10 minutes. Later, Na_2S solution was added dropwise into the solution of $CdSO_4$. This solution mixture was kept on stirring for 20 minutes. The whole process was carried out at room temperature without the addition of any capping agent. Wet yellow precipitates were obtained as the resultant product. After the centrifugation process, these precipitates were dried in an oven at 80°C for 48 hours [10].

Synthesis of pure PMMA film

Pure poly methyl methacrylate (PMMA) film was prepared by dissolving 1g of PMMA in 20 mL of chloroform at room temperature and kept on stirring until a clear solution was obtained. Later, the solution was poured into a petri dish for the evaporation of solvent [21].

Synthesis of CdS/PMMA composites

For the formation of thin films of CdS/PMMA composites, different amounts of CdS nanoparticles were added in a constant amount of PMMA solution, separately. In the first step, 1g of PMMA was dissolved in 20 mL of chloroform and kept on constant stirring until the formation of a clear solution. A specific amount of CdS nanoparticles was added to this solution and stirring was continued for a further 20 minutes. Afterward, to obtain the homogeneous suspension, this mixture was sonicated for 30 minutes in an ultra-sonicated bath. Finally, the suspension was poured into a petri dish for solvent evaporation at room temperature [22]. Different films of CdS/PMMA were prepared by varying the amount of nanoparticles in 1 g of PMMA matrix as shown in Table 1.

Table 1. Composition of CdS/PMMA nanocomposites

Nanocomposite Name	Composition
Sample A	0.1 g of CdS / 1 g PMMA
Sample B	0.4 g of CdS / 1 g PMMA
Sample C	0.6 g of CdS / 1 g PMMA
Sample D	0.8 g of CdS / 1 g PMMA
Sample E	1 g of CdS / 1 g PMMA
Sample F	1.2 g of CdS / 1 g PMMA

Photocatalytic activity

For the photodegradation of methylene blue (MB), CdS/PMMA films were used as photocatalysts at room temperature in the presence of an artificial visible light source of 40 W. Photocatalytic activities were observed by mixing CdS/PMMA composites, with different quantities of CdS, in 100 mL of aqueous solution of MB ($1x10^{-4}$ M), separately at constant stirring. During stirring, 1μL of barium hydroxide (0.06M) was added to this solution to maintain the pH of the solution at 10. This solution was kept on stirring for 4 hours and the degradation of dye was studied periodically after different time intervals with the help of a UV-Visible spectrophotometer. As concentration is directly proportional to absorbance the degradation efficiency of MB can be calculated with the help of the following equation (1), [23]:

$$Degradation\,Efficiency = E = \frac{C_o - C}{C_o} X\,100 = \frac{A_o - A}{A_o} X\,100 \qquad (1)$$

Here, C_o, C, A and A_o are the concentrations and absorbance of MB at 0 and t time of reaction, respectively. Similarly, with the help of the following equation (2):

$$ln\frac{C}{C_o} = kt \qquad (2)$$

Where t is illumination time and k is the first-order rate constant, the rate of reaction was calculated by plotting a graph between ln C/Co and time [23].

Results and Discussion

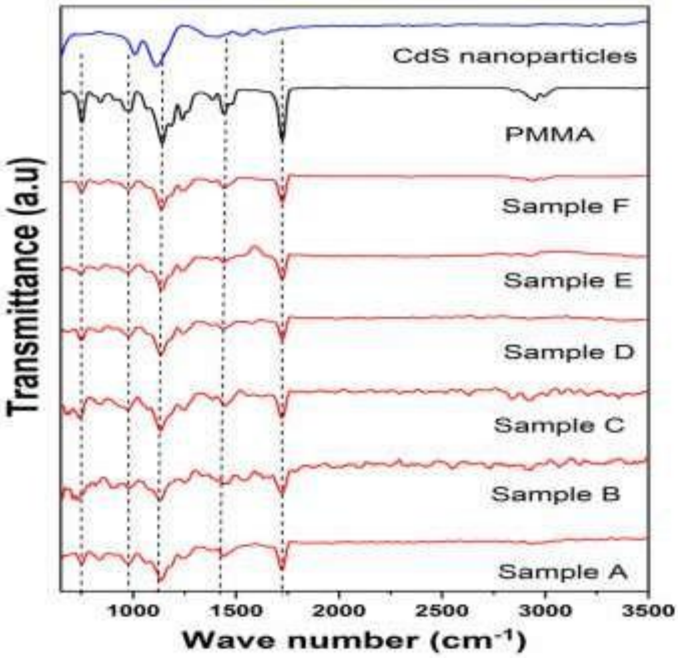

Figure 1. FTIR spectra of different compositions of CdS /PMMA composites, pure PMMA and pure CdS nanoparticles

Figure 1 shows the FTIR spectra of pure PMMA, pure CdS nanoparticles and different compositions of CdS/PMMA nanocomposites from sample A to sample F respectively. There are usually two regions in the FTIR spectrum named as functional group region (range from 4000 to 1500cm^{-1}) and fingerprint region (range from 1500 to 400 cm^{-1}.). FTIR Spectrum of pure PMMA showed stretching vibration for the C=O group at 1728 cm^{-1}, bending vibrations for the C-O group between 1075 to 1274 cm^{-1}, and a peak at 1442 corresponds to the bending vibrations for the O-CH$_3$ group [22,24,25]. The peak at 756 cm^{-1} appeared due to the vibration in polymer chains [26] peak at 841 cm^{-1} is attributed to the bending vibrations of the C-H group [27]. FTIR spectra of pure PMMA and those of CdS/PMMA nanocomposites are almost the same. It is reported that CdS nanoparticles with a maximum 3 % (0.045 g) weight percent in solution, do not disturb the continuous 3-D network of PMMA matrices and both matrices and fillers kept their independent chemical properties [27].

Pristine PMMA is a transparent polymer with low transmission of light in the ultraviolet region. This transparency decreases as the amount of CdS is increased in the PMMA matrix. CdS is a direct band gap (n-type photo sensible) semiconductor and its conduction band minimum and valence band maximum lie at the same momentum. It means that the transition of electrons takes place directly between these bands at the same momentum (K=0) and makes the process of absorption and emission more effective. The direct band gap value of CdS is 2.4 eV [9,10]. To determine the optical properties of CdS/PMMA composites, direct band gap energy *(E_g)* was calculated by plotting the graph between "$(\alpha h\nu)^2$" verses "$h\nu$" (as shown in Figure.2) by following equation (4) [23,24];

$$(\alpha h\nu)^2 = B(h\nu - E_g) \qquad (4)$$

Here, "α" represents the coefficient of absorption and is equal to *2.303(A/t)* (where *A* represents the absorption or optical density and *t* represents the cuvette's path length: which is equal to 1cm in the present case), B is a constant and "$h\nu$" represents the energy of photon [23]. Differences in band gap energy of different samples of CdS/PMMA composites with respect to pristine PMMA are shown in Table 2 as follows:

Table 2. Band gap energy differences of different composites of CdS/PMMA with respect to pure PMMA

Sample Name	**Band gap energy (eV)**	**Band gap energy difference with respect to pure PMMA**
Pure PMMA	4.31	-
Sample A	3.88	0.43
Sample B	3.01	1.30
Sample C	2.56	1.75
Sample D	2.39	1.92
Sample E	2.31	2.00
Sample F	2.30	2.01

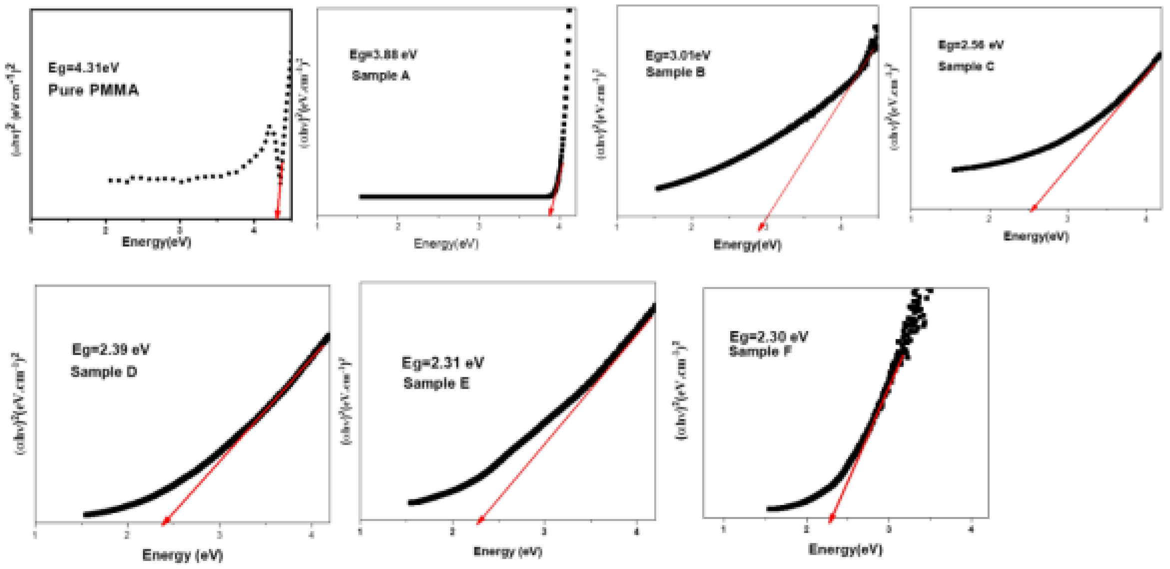

Figure 2. Tauc plots of pure PMMA and its composites with different compositions of CdS nanoparticles

The band gap energy observed for PMMA is 4.31 eV and to make it useful for different optical applications, its band gap energy can be tuned by integrating any conducting material into it. The incorporation of materials like CNTs or semiconducting nanoparticles may introduce new electronic states in the PMMA matrix and result in narrowing the band gaps and enhancing the electrical properties [28]. Table 2 shows the band gap energy values of pure PMMA and its composites with different concentrations of CdS nanoparticles. The subsequent decrease in band gap energy of PMMA upon increasing the amount of CdS depicts that the incorporation of CdS into the PMMA matrix is increased gradually by developing the strong interaction between the electronic states of CdS and the polymeric structure of PMMA [24,29]. The same is depicted in Figure 3, the broadness of the pure PMMA peak is subsequently changed into a sharp one that reflects the uniform distribution of CdS nanoparticles in the matrix. It is noteworthy here, that as the nanoparticles are uniformly distributed each CdS nanoparticle has the chance to interact with light individually and leads towards the decrease in band gap energy of the PMMA matrix [30].

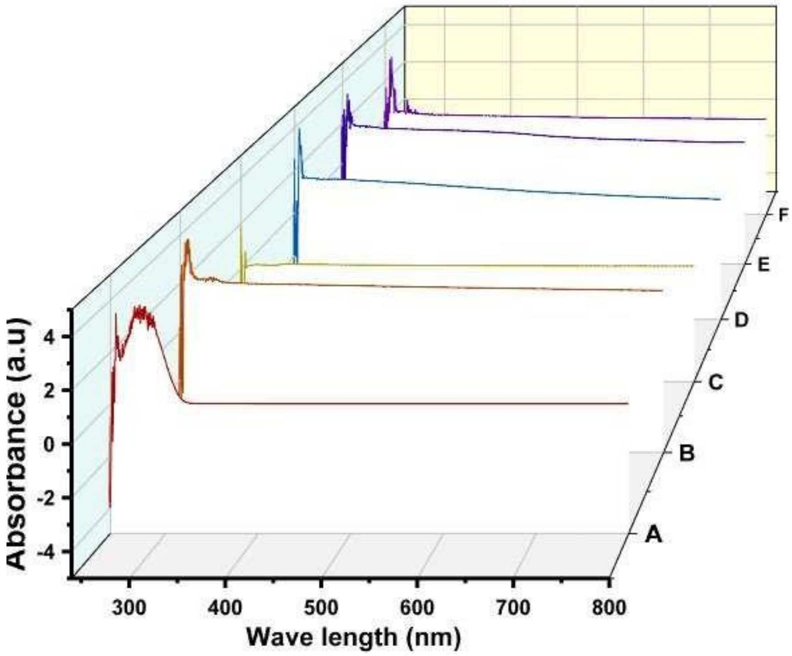

Figure 3. UV-Visible spectra of Cd/PMMA composites with different wt.% of CdS in PMMA matrix

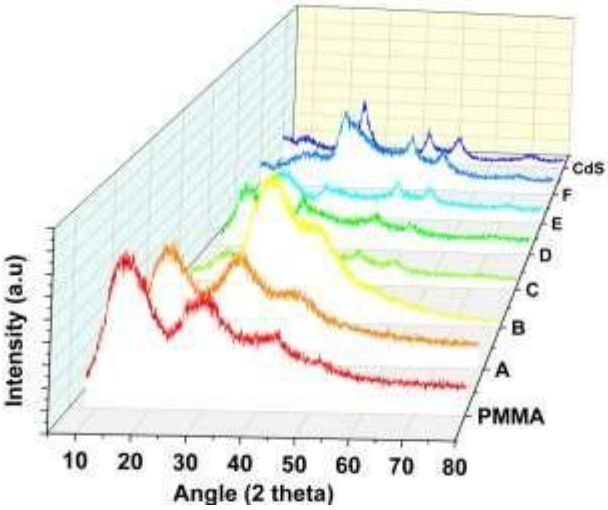

Figure 4. XRD patterns of PMMA, CdS and composites of CdS/PMMA composites with different contents of CdS nanoparticles

XRD patterns of pure PMMA, CdS and different composites of CdS/PMMA are shown in Figure 4. Characteristic 2 theta peaks obtained for pure PMMA are present at 14.9^{o}, 30.5^{o} and 43.4^{o} and 26.4^{o}, 43.6^{o}, 51.5^{o} for pure CdS. These results are well matched with the previous studies as well like XRD pattern as reported for CdS nanoparticles indicated the 2 theta values at 26.54^{o}, 43.52^{o} and 51.49^{o} with (111), (220) and (311) cubic phase plans of CdS, respectively [18]. Similarly, peaks of pure PMMA are close to the ones reported in the literature [18,24]. In the cases of CdS/PMMA composites, an increase in the broadness of peaks of CdS in the PMMA matrix is observed representing the increase in the roughness of the system due to the incorporation of CdS nanoparticles in the polymeric structure. This surface roughness is increased as the concentration of the CdS nanoparticles is increased because these particles may have started developing a chain-like network/agglomerates in the system upon increasing the concentration [31].

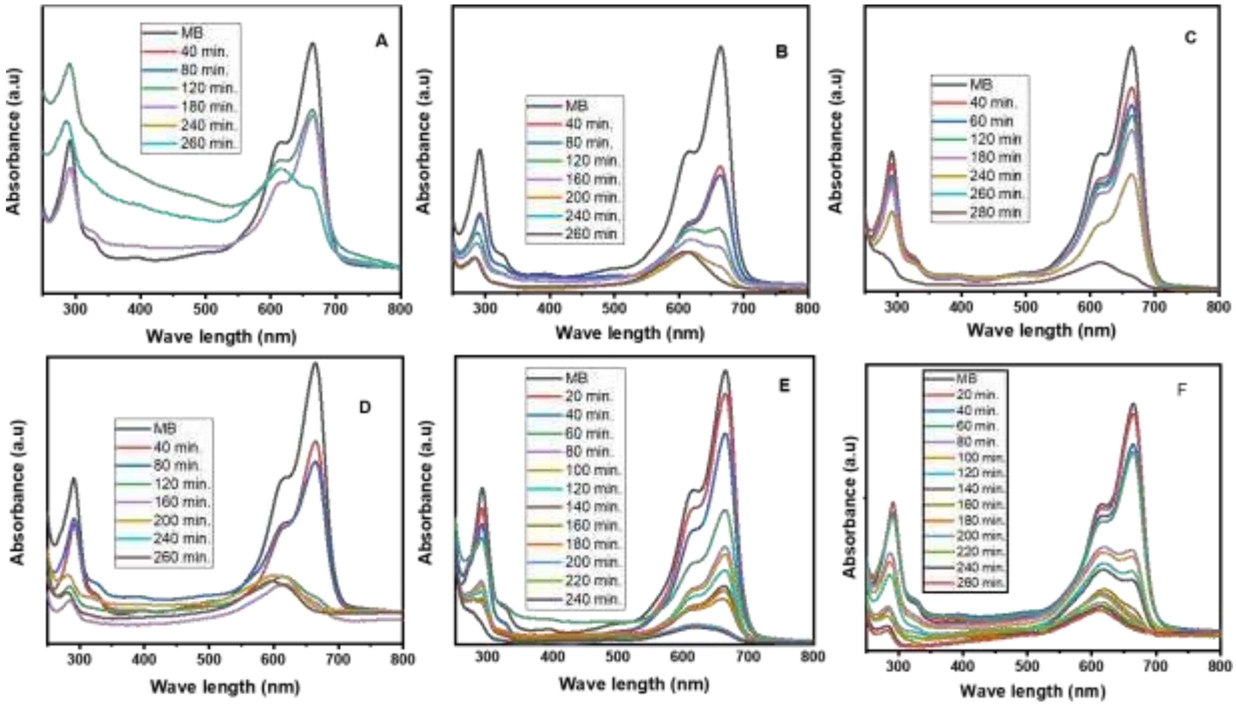

Figure 5. Photodegradation of MB by using different CdS/PMMA nanocomposites

The effect of the catalyst against MB was investigated under visible irradiation, at λ max equals to 665 nm, by using different thin films of CdS/PMMA nanocomposites. Figure 5 shows that as the amount of CdS was increasing the interaction of the molecules of MB with CdS was increased. The maximum interaction is observed for sample D and a significant decrease in absorbance is observed as the light irradiation time was increased. However, as the amount of CdS nanoparticles was increased, this sharp effect slowed down and it may be suggested here, that at higher concentrations, the availability of free charges and defects in PMMA matrix may have decreased. Figure 6 shows the plot between ln C/C_o and different irradiation times. This plot helps to calculate the values of the rate of reactions as its slope gives the value of rate constant "k" and the square of the correlation coefficient of linear fit (R^2). The % removal of MB at different irradiation times is shown in Figure 7. Near 40 minutes all the samples showed significant thresholds in the removal of MB that show the availability of free charges on CdS and pores on the surface of the PMMA matrix. However, with increasing time between 50-100 minutes sample D showed a different behavior, first a significant increase in the threshold of % removal of MB and after that, it showed a slow or almost close to equilibrium state. This behavior of sample D shows that till 100 minutes, free charges and defects were sufficiently available for the molecules of MB to react with CdS nanoparticles in the presence of UV light, however, when the reaction became fast the availability of free charges on CdS and defects in the PMMA matrix decreases and therefore this sample slowed down its further reaction and almost became constant at the end. The behavior of other samples was somehow slow as compared to sample D. In Figure 8, the difference between the values of R^2 and k can easily be observed. For sample A the values of k and R^2 are 0.00363 min^{-1} and 83, for sample B: 0.01602 min^{-1} and 0.95, for sample C: 0.0093 min^{-1} and 0.65, sample D: 0.02361 min^{-1} and 0.96, for sample E: 0.01494 min^{-1} and 0.94 and for sample D: 0.01707 min^{-1} and 0.98. The rate of reaction increases (sample A < Sample B ~ sample C< sample D > sample E < sample F) as the amount of CdS was increased in the PMMA matrix but after sample D, the reaction rate became slightly slow in sample E and F which may be due to some sort of agglomeration among the CdS nanoparticles that may hinder the interaction of MB molecules.

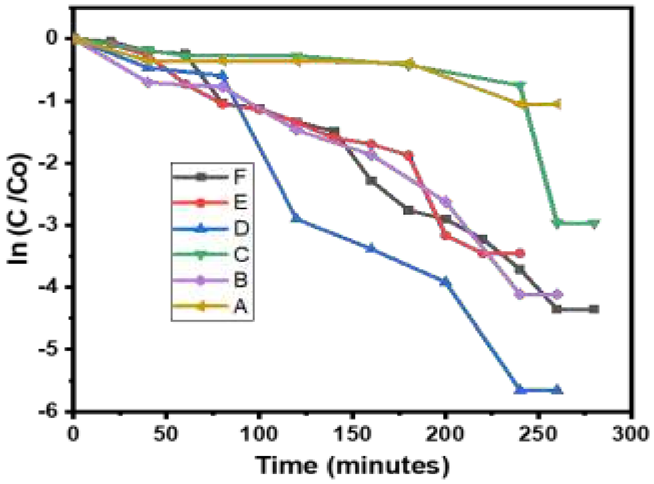

Figure 6. Plot between ln C /C_o and irradiation time intervals

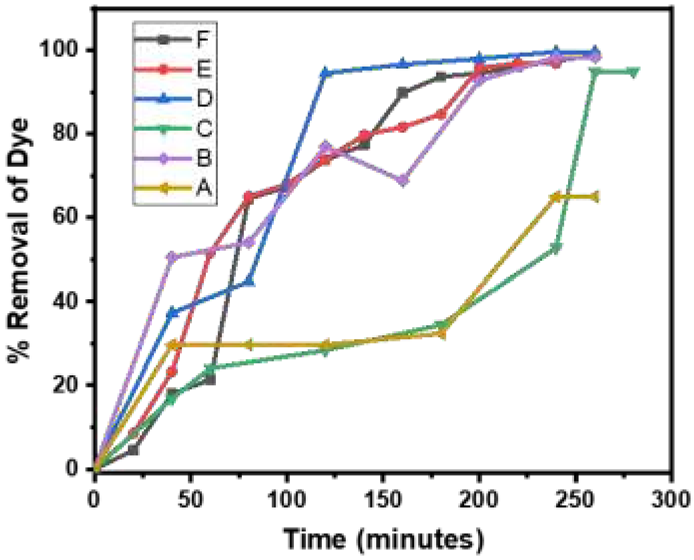

Figure 7. %removal efficiency of CdS/PMMA nanocomposites at different time intervals

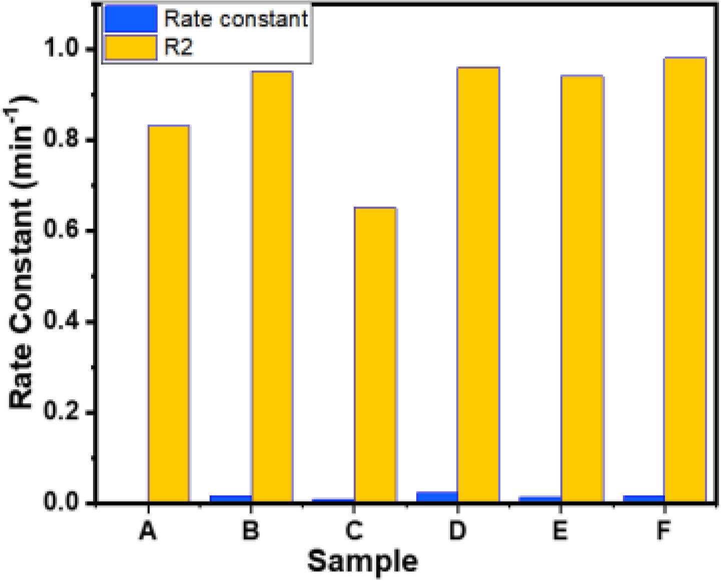

Figure 8. Kinetic rate constants and square of correlation coefficient of different samples of CdS/PMMA composites

Overall, the incorporation of CdS into the PMMA matrix affected the photodegradation of MO significantly. CdS nanoparticles possess narrow band gap energy and could be used as strong photocatalysts. When these nanoparticles are exposed to light (hν) they absorb photons and cause the excitation of the electrons (e-) present in their conduction band to the valence band by leaving holes (h+) behind at their places. These e- and h+ pairs are the initiators of the redox reactions required for the photodegradation of MB. On the other hand, the PMMA matrix provides a platform where these nanoparticles can be dispersed uniformly and reduce the recombination of e- and h+ pairs upon irradiation with light. In Figure 3, the sharpness of the UV-Visible peaks affirms the uniform distribution of nanoparticles in the PMMA matrix with a higher surface area that increases the chances of more interaction of nanoparticles with light and dye molecules. The e- present in the conduction band reduces the dissolved oxygen (present in the aqueous solution of MB) and converts it into superoxide radicals ($*O^{-2}$). On the other hand, the h+ present in the valence band produces hydroxyl radicals (^-OH) by oxidizing the water molecules or hydroxyl ions (^-OH). Both of these radicals ($*O^-_2$, $*OH$) are known as reactive oxygen species (ROS). These ROS react with the molecules of MB and break them into CO_2 and H_2O. Equations (5) to (11) show the reactions that occur between the CdS/PMMA catalyst and aqueous solution of MB under the irradiation of light (hν) [18,30].

$$\text{CdS/PMMA} + h\nu \rightarrow e^-_{CB} + h^+_{VB} \qquad (5)$$

$$e^-_{CB} + O_2 \rightarrow *O^-_2 \qquad (6)$$

$$*O^-_2 + H_2O \rightarrow H_2O* + {}^-OH \qquad (7)$$

$$*O^-_2 + H_2O* \rightarrow H_2O_2 + O_2 \qquad (8)$$

$$h^+_{VB} + {}^-OH \rightarrow *OH \qquad (9)$$

$$h^+_{VB} + H_2O \rightarrow H^+ + *OH \qquad (10)$$

$$*OH + MB \rightarrow \text{Degradation product} / CO_2 + H_2O \qquad (11)$$

Table 3. Comparison of different nanocomposites, their % removal of dye and time duration

Composite	Wt%	Degradation %	Time	Reference
Sample A	0.1 g	65 %	240 minutes	Present work
Sample B	0.4 g	98 %	240 minutes	
Sample C	0.6 g	94 %	260 minutes	
Sample D	0.8 g	99 %	240 minutes	
Sample E	1 g	97 %	220 minutes	
Sample F	1.2 g	98 %	260 minutes	
ZnO/PMMA	2.5 g	100 %	80 minutes	[30]
TiO_2(0D)/PMMA & TiO_2(1D)/PMMA	5 g 5 g	28.8 % 18 %	4 hours	[32]
Graphene-SnO_2/PMMA	0.1 g	99 %	60 minutes	[33]
TiO_2/PMMA	Sprinkled TiO_2	30 %	200 minutes	[34]

Table 3 shows the comparison of the present work with the recent research done by incorporating different nanoparticles into the PMMA matrix. From the present investigation, it may be stated that each nanoparticle creates a different atmosphere within the polymer structure and thus the availability of free charges and spaces varies. When the CdS/PMMA composite was used for the removal of RhB from aqueous water, it degraded the 100 % dye in just 30 minutes [18]. On the other hand, in another research, when CdS/PMMA was treated as a photocatalyst for the degradation of MB, methyl orange (MO) and RhB, three days were taken and only 36 % MB, 80 % MO and 90 % RhB were degraded [35]. CdS and PMMA both possess tunable properties which make them useful in several applications like the one studied in present research.

Conclusion

Nanoparticles of CdS (0.1 g, 0.4 g, 0.6 g, 0.8 g, 1 g and 1.2 g) were incorporated in each 1 g of PMMA polymer structure by solution casting method. These thin films were characterized by using Hi-tech instruments like FTIR, UV-visible spectroscopy and XRD. FTIR analysis showed that the incorporation of CdS nanoparticles did not disturb the polymer structure of PMMA. The band gap energy values of PMMA were decreased as the amount of CdS was increased. The XRD pattern showed an increase in the peak broadness which depicts that the smoothness of the PMMA surface is enhanced with the addition of CdS. Composite of CdS /PMMA thin film with 0.8 g of CdS showed 99 % degradation of MB in 240 minutes whereas a sharp degradation jump was observed in just 120 minutes with 94 % removal of dye. These fabricated thin films can be investigated to find the synergetic impact of CdS on the electrical and thermal properties of the PMMA matrix so that these films can be used in electronic industries as well.

Credit Author Statement

Conceptualization, literature review, methodology, analysis and result interpretation were done equally by Huma Tareen and Dr. Farrukh Bashir, whereas, drafting, editing, result discussion and reviewing were done by **Dr. Irum Javid, Dr. Naheed Sajjad, Dr. Zile Huma, Muhammad Riaz, Khurrum Shazad Buzdar, and Muhammad Aamir Raza.**

Conflict of interest

The authors affirm the absence of any conflicting interests.

References

1. Ghahestani, S.M.; Shahab, E.; Karimi, S.; Madani, M.H. Methylene blue may have a role in the treatment of COVID-19. *Medical Hypotheses* **2020**, *144*, 110163, doi:https://doi.org/10.1016/j.mehy.2020.110163.
2. Bužga, M.; Machytka, E.; Dvořáčková, E.; Švagera, Z.; Stejskal, D.; Máca, J.; Král, J. Methylene blue: a controversial diagnostic acid and medication? *Toxicology Research* **2022**, *11*, 711-717, doi:10.1093/toxres/tfac050.
3. Houas, A.; Lachheb, H.; Ksibi, M.; Elaloui, E.; Guillard, C.; Herrmann, J.-M. Photocatalytic degradation pathway of methylene blue in water. *Applied Catalysis B: Environmental* **2001**, *31*, 145-157.
4. Singh, J.; Chang, Y.-Y.; Koduru, J.R.; Yang, J.-K. Potential degradation of methylene blue (MB) by nano-metallic particles: A kinetic study and possible mechanism of MB degradation. *Environmental Engineering Research* **2018**, *23*, 1-9.
5. Liu, T.; Yang, G.; Wang, W.; Wang, C.; Wang, M.; Sun, X.; Xu, P.; Zhang, J. Preparation of C3N5 nanosheets with enhanced performance in photocatalytic methylene blue (MB) degradation and H2-evolution from water splitting. *Environmental Research* **2020**, *188*, 109741.
6. Upendar, G.; Dutta, S.; Bhattacharya, P.; Dutta, A. Bioremediation of methylene blue dye using Bacillus subtilis MTCC 441. *Water Science and Technology* **2017**, *75*, 1572-1583.
7. Bharti, V.; Vikrant, K.; Goswami, M.; Tiwari, H.; Sonwani, R.K.; Lee, J.; Tsang, D.C.; Kim, K.-H.; Saeed, M.; Kumar, S. Biodegradation of methylene blue dye in a batch and continuous mode using biochar as packing media. *Environmental research* **2019**, *171*, 356-364.
8. Ahmad, A.; Singh, A.P.; Khan, N.; Chowdhary, P.; Giri, B.S.; Varjani, S.; Chaturvedi, P. Bio-composite of Fe-sludge biochar immobilized with Bacillus Sp. in packed column for bio-adsorption of Methylene blue in a hybrid treatment system: Isotherm and kinetic evaluation. *Environmental Technology & Innovation* **2021**, *23*, 101734.
9. Sheng, C.K.; Amin, K.A.M.; Hong, L.L.; Hassan, M.F.; Ismail, M. Investigation of morphological, structural and electrical properties of Cds/PMMA nanocomposite film prepared by solution casting method. *Int. J. Electrochem. Sci* **2017**, *12*, 10023-10031.
10. Bangi, U. Impact of cadmium salt concentration on CdS nanoparticles synthesized by chemical precipitation method. *Chalcogenide Letters* **2020**, *17*, 537-547.

11. Pandian, S.R.K.; Deepak, V.; Kalishwaralal, K.; Gurunathan, S. Biologically synthesized fluorescent CdS NPs encapsulated by PHB. *Enzyme and microbial technology* **2011**, *48*, 319-325.
12. Brown, J.W.; Ramesh, P.; Geetha, D. Photodegradation of Methylene Blue Dye Using Nanocomposites of Copper Sulfide Doped with Fe/Cd/Zr as Nanophotocatalyst. *Indian Journal of Science and Technology* **2019**, *12*, 45.
13. Osuntokun, J.; Ajibade, P.A. Structural and thermal studies of ZnS and CdS nanoparticles in polymer matrices. *Journal of Nanomaterials* **2016**, *2016*.
14. Kumar, S.; Sharma, J. Stable phase CdS nanoparticles for optoelectronics: a study on surface morphology, structural and optical characterization. *Materials Science-Poland* **2016**, *34*, 368-373.
15. Mahanthappa, M.; Kottam, N.; Yellappa, S. Enhanced photocatalytic degradation of methylene blue dye using CuSCdS nanocomposite under visible light irradiation. *Applied Surface Science* **2019**, *475*, 828-838.
16. Jang, J.; Kim, S.; Lee, K.J. Fabrication of CdS/PMMA core/shell nanoparticles by dispersion mediated interfacial polymerization. *Chemical communications* **2007**, 2689-2691.
17. Zhong, W.; Tu, W.; Wang, Z.; Lin, Z.; Xu, A.; Ye, X.; Chen, D.; Xiao, B. Ultralow-temperature assisted synthesis of single platinum atoms anchored on carbon nanotubes for efficiently electrocatalytic acidic hydrogen evolution. *Journal of Energy Chemistry* **2020**, *51*, 280-284.
18. Hussien, M.S.; Mohammed, M.I.; Yahia, I.S. Flexible photocatalytic membrane based on CdS/PMMA polymeric nanocomposite films: multifunctional materials. *Environmental Science and Pollution Research* **2020**, *27*, 45225-45237.
19. Padmaja, S.; Jayakumar, S. Tunable luminescence and transmittance nature of CdS: PMMA nanocomposites for optoelectronic applications. *Optics & Laser Technology* **2019**, *112*, 409-412.
20. Pedone, L.; Caponetti, E.; Leone, M.; Militello, V.; Pantò, V.; Polizzi, S.; Saladino, M.L. Synthesis and characterization of CdS nanoparticles embedded in a polymethylmethacrylate matrix. *Journal of colloid and interface science* **2005**, *284*, 495-500.
21. Hussain, T.; Bashir, F.; Mujahid, A.; Intisar, A.; Ahmad, M.N.; Raza, M.A.; Din, M.I.; Jabeen, U.; Mushtaq, A.; Tareen, H. Highly Stable APTES Incorporated CNTs Based Ternary Polymer Composites with Improved Dielectric and Thermal Properties. *Silicon* **2022**, 1-10.
22. Bashir, F.; Hussain, T.; Mujahid, A.; Shehzad, K.; Raza, M.A.; Zahid, M.; Athar, M.M. Tailoring electrical and thermal properties of polymethyl methacrylate-carbon nanotubes composites through polyaniline and dodecyl benzene sulphonic acid impregnation. *Polymer Composites* **2018**, *39*, E1052-E1059.
23. Soltani, N.; Saion, E.; Yunus, W.M.M.; Navasery, M.; Bahmanrokh, G.; Erfani, M.; Zare, M.R.; Gharibshahi, E. Photocatalytic degradation of methylene blue under visible light using PVP-capped ZnS and CdS nanoparticles. *Solar Energy* **2013**, *97*, 147-154.
24. Bashir, F.; Hussain, T.; Mujahid, A.; Mushtaq, A.; Raza, M.A.; Ahmad, M.N.; Zahid, M.; Din, M.I.; Tareen, H. Zwitterionic surfactant modified carbon nanotubes incorporated percolative polymer composites with improved features. *Nano Biomedicine & Engineering* **2023**, *15*.
25. Hussain, T.; Bashir, F.; Mujahid, A.; Intisar, A.; Ahmad, M.N.; Raza, M.A.; Din, M.I.; Jabeen, U.; Mushtaq, A.; Tareen, H. Highly Stable APTES Incorporated CNTs Based Ternary Polymer Composites with Improved Dielectric and Thermal Properties. *Silicon* **2022**, *14*, 10807-10816.
26. Hussain, T.; Ahmad, M.N.; Nawaz, A.; Mujahid, A.; Bashir, F.; Mustafa, G. Surfactant incorporated Co nanoparticles polymer composites with uniform dispersion and double percolation. *Journal of Chemistry* **2017**, *2017*.
27. Mbese, J.Z.; Ajibade, P.A. Preparation and Characterization of ZnS, CdS and HgS/Poly(methyl methacrylate) Nanocomposites. *Polymers* **2014**, *6*, 2332-2344.
28. Bashir, F.; Hakeem, P.; Mushtaq, A.; Tareen, H.; Aamir, M.; Buzdar, K.S. Role of Metallic and Bimetallic Modified Carbon Nanotubes in the Formation of Polymethyl Methacrylate Composites: Zn-CNTs and Cu-Zn/CNTs based PMMA composites. *Pakistan Journal of Multidisciplinary Research* **2023**, *4*, 32-45.

29. Al-Bataineh, Q.M.; Ahmad, A.A.; Alsaad, A.; Telfah, A.D. Optical characterizations of PMMA/metal oxide nanoparticles thin films: bandgap engineering using a novel derived model. *Heliyon* **2021**, *7*.
30. Mohammed, M.; Khafagy, R.; Hussien, M.S.; Sakr, G.; Ibrahim, M.A.; Yahia, I.; Zahran, H. Enhancing the structural, optical, electrical, properties and photocatalytic applications of ZnO/PMMA nanocomposite membranes: Towards multifunctional membranes. *Journal of Materials Science: Materials in Electronics* **2021**, 1-26.
31. Trabelsi, A.B.G.; Mostafa, A.M.; Alkallas, F.H.; Elsharkawy, W.; Al-Ahmadi, A.N.; Ahmed, H.A.; Nafee, S.S.; Pashameah, R.A.; Mwafy, E.A. Effect of CuO nanoparticles on the optical, structural, and electrical properties in the PMMA/PVDF nanocomposite. *Micromachines* **2023**, *14*, 1195.
32. Morales, G.; Astrid Yáñez-Hernández, L.; Lozano, K.; Padilla-Gainza, V.; Alejandro Lozano-Morales, S. Photocatalytic degradation of methylene blue using PMMA/TiO2 nanoparticles composites fibers obtained through centrifugal spinning. *International Journal of Environmental Science and Technology* **2024**, *21*, 4611-4624.
33. Shanmugam, M.; Alsalme, A.; Alghamdi, A.; Jayavel, R. Photocatalytic properties of graphene-SnO2-PMMA nanocomposite in the degradation of methylene blue dye under direct sunlight irradiation. *Materials Express* **2015**, *5*, 319-326.
34. Ounas, O.; El Foulani, A.A.; Lekhlif, B.; Jamal-Eddine, J. Immobilization of TiO2 into a poly methyl methacrylate (PMMA) as hybrid film for photocatalytic degradation of methylene blue. *Materials Today: Proceedings* **2020**, *22*, 35-40.
35. Liu, F.; Han, C.; Sun, P.; Wang, G.; Li, J.; Chang, Q. Spherical CdS Nanoparticles Precipitated from a Cadmium Thiosulfate Complex Using Ultraviolet Light for Photocatalytic Dye Degradation. *Metals* **2023**, *13*, 554.